Mining, Metallurgy & Exploration (2022) 39:1087–1098
https://doi.org/10.1007/s42461-022-00580-6

Fire Size and Response Time Predictions in Underground Coal Mines Using Neural Networks

Manuel J. Barros-Daza[1,3] · **Kray D. Luxbacher**[1] · **Brian Y. Lattimer**[2] · **Jonathan L. Hodges**[3]

Received: 20 July 2021 / Accepted: 6 March 2022 / Published online: 23 March 2022

Abstract
The prediction of the coal mine fire response time, defined as the remaining time before conditions at attack positions grow untenable for firefighters, plays a vital role in the decision-making process during a mine fire scenario. The knowledge of the response time along with the fire size, fire location, and arrival time could allow for the most suitable decision regarding direct or remote approach to the fire in the mine, mine evacuation planning, and remote attack from the surface. For this reason, this paper presents a data-driven approach to predict the response time and fire size based on available and measurable parameters during underground coal mine fires using two interconnected artificial neural networks (ANNs). A total of 300 fire dynamic simulator (FDS) and fire and smoke simulator (FSSIM) simulations of a straight and flat mine entry (replicating a belt entry) with different fire sizes, air velocities, and dimensions were used in training and testing the ANNs. The results showed that 95% of fire size and response time predictions should be within ± 29 kW and ± 4 s of true values obtained in the fire models, respectively. The approach presented in this work can provide instantaneous predictions of response time and fire size during ongoing mine fires. Additionally, this approach can be utilized in other mine fire locations as well as in different types of tunnels.

Keywords ANN neural network · Mine firefighters · Response time · Fire size

1 Introduction

Once a fire is discovered in an underground coal mine, a decision-making aims to reduce the probability of high-risk event. Among these options is the possibility of attacking the fire directly or through remote techniques when conditions are not tenable for the firefighting personnel. In most underground mine fires, direct attack at the initial stages is usually a priority since fires develop rapidly. If a fire cannot be controlled by direct firefighting methods, the probability of effectively extinguishing the fire without the need to seal the mine or a portion of the mine is greatly reduced [1–4]. However, considering the accessibility of coal mines and the potential remote locations of fires, some fires cannot be attacked during their first stages. Conditions at the fire proximity can grow untenable preventing firefighters' approach to carry out direct attack. Thus, predictions of the evolution of the conditions in the proximity of the fire could allow for the determination of the response time defined as the remaining time before conditions at attack positions become untenable for firefighters. The determination of the response time along with the knowledge of the fire size, fire location, and arrival time allows for the most informed and methodical decision regarding the type of attack. These decisions must be made relatively quickly, so there is a need for a new approach that can determine the response time and fire size in real time during ongoing mine fire scenarios. This approach must use measurable and available parameters in underground coal mines in order that it can be applied in the field.

To predict the conditions generated by enclosed fires such as in underground mines, two types of models have been used: computational fluid dynamics (CFD) fire models and zone fire models (ZFM) [4–9]. In CFD fire models the Navier–Stokes equations of mass, momentum, and energy

✉ Manuel J. Barros-Daza
manuel1@vt.edu

[1] Virginia Tech (Mining and Minerals Engineering), Blacksburg, VA, USA

[2] Virginia Tech (Mechanical Engineering), Blacksburg, VA 24061, USA

[3] Jensen Hughes, 2020, Kraft Drive, Suite 3020, Blacksburg, VA 24060, USA

are solved as well as the species conservation equation in discretized geometries allowing for the spatial–temporal resolution of the entire domain. Parameters such as concentrations of combustion gasses, temperature, visibility, and radiation in each grid cell are solved. However, the high computational cost and processing time of these models that can be in order of days or even weeks makes it impractical to use in informing real-time conditions. On the other hand, in zone fire models the domain is divided into larger compartments which are represented as single nodes [10]. This approach of having one node per control volume minimizes the computational cost and time allowing for faster predictions of smoke spread in larger domains. Although zone fire model simulations can be obtained much faster than CFD models, it is still unfeasible to solve entire domains and process results in real time. In addition, it is noteworthy that ZFM predictions have low spatial resolution for hazard analysis.

Advancements in machine learning and improvements in computing power have contributed to an increase in the usage of artificial neural networks (ANNs) for development of data-driven models able to solve domains and process results in real time [11–17]. ANNs can learn complex dependencies between variables which makes them an attractive technology for this kind of application. For instance, Hodges et al. [17] recently used machine learning to approximate the detailed thermal flow field in a mine fire showing the capability of ANNs to predict conditions in underground mines. Nevertheless, this study did not focus on evaluation of atmosphere conditions nor calculation of response time and fire size. An approach which uses measurable and available parameters as inputs to a machine learning model to determine response time and fire size in real time is particularly promising for decision-making during fire emergency response.

The objective of this study was to develop a data-driven model to make predictions of response times and fire sizes in real time based on on-site CO concentration sensor readings downwind from the fire and other known operating parameters such as mine geometry, air velocity, and time elapsed after fire detection. This approach was implemented for different fire scenarios in a straight and flat mine entry (replicating a belt entry) with different fire characteristics, air velocities, and dimensions. The data used for training and testing the data-driven approach was generated using a CFD model called fire dynamics simulator (FDS) and a zone fore model called fire and smoke simulator (FSSIM). FDS was used for the determination of conditions in the proximity of the fire where the attack position is located. FSSIM was used to determine CO concentrations downwind from the fire. The entire model was composed of two interconnected feedforward ANNs in which the prediction of the fire size performed by the first ANN is used by the second ANN to predict the response time. The approach presented in this work can provide instantaneous predictions of fire size and response time during ongoing mine fires and be applied to other mine fire locations as well as in different types of tunnels.

2 Methodology

A sketch showing a high-level view of the solution algorithm used to develop the data-driven approach for prediction of fire size and response time is shown in Fig. 1. ANN-1 makes predictions of fire size using input parameters measured in mines. Fire size predictions by ANN-1 along other operating parameters are used as input to ANN-2 for response time determination. Data for training and testing ANNs was generated using FDS and FSSIM simulations. A tenability analysis was performed for calculation of response time in different scenarios. The following subsections describe the network architecture, tenability analysis, and data generation and preparation used in this work.

2.1 Network Architectures

The entire model for the determination of fire size and response time used in this study is composed of two interconnected ANNs as shown in Fig. 1. The main constraint for the elaboration of the predictive model was to use only available and measurable parameters during underground coal mine fires as inputs to the ANNs. According Title 30 CFR §75.351(e)(f)(h), underground coal mines are required to be monitored of carbon monoxide by atmospheric monitoring systems (AMS) or CO systems [18]. As defined in

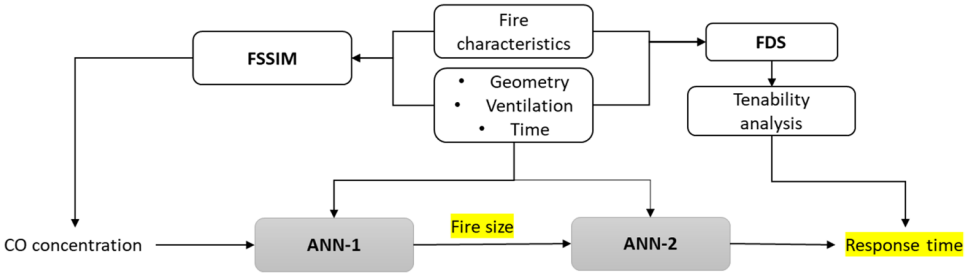

Fig. 1 Sketch of solution algorithm

Title 30 CFR §75.301, AMS or CO systems are described as networks consisting of hardware and software capable of measuring atmospheric parameters and transferring the measurements to a designated surface location. For CO monitoring, sensors of these systems must be located at key locations such as belt and return entries, working faces, electrical installation locations, and primary escapeways. This indicates that during mine fires, CO concentration is measured at different mine locations and transmitted to surface in real time in all US underground coal mines. CO is a combustion product which its concentration contains information of the fire size and conditions during ongoing mine fire. Thus, CO concentration was selected as one of the input parameters to the predictive model. In addition to CO concentration, there are known operating parameters that can impact fire conditions. These known parameters are mine entry dimensions, time elapsed after fire detection, and nominal longitudinal air velocity. They are all known since they are part of the mine operating procedures. These additional parameters were used along with CO concentration as input parameters to the ANNs (Figs. 2,3 and 4).

The architecture of the first ANN (ANN-1) consists of fully connected layers of which three are hidden layers of 30 neurons as shown in Fig. 5. The input layer is composed

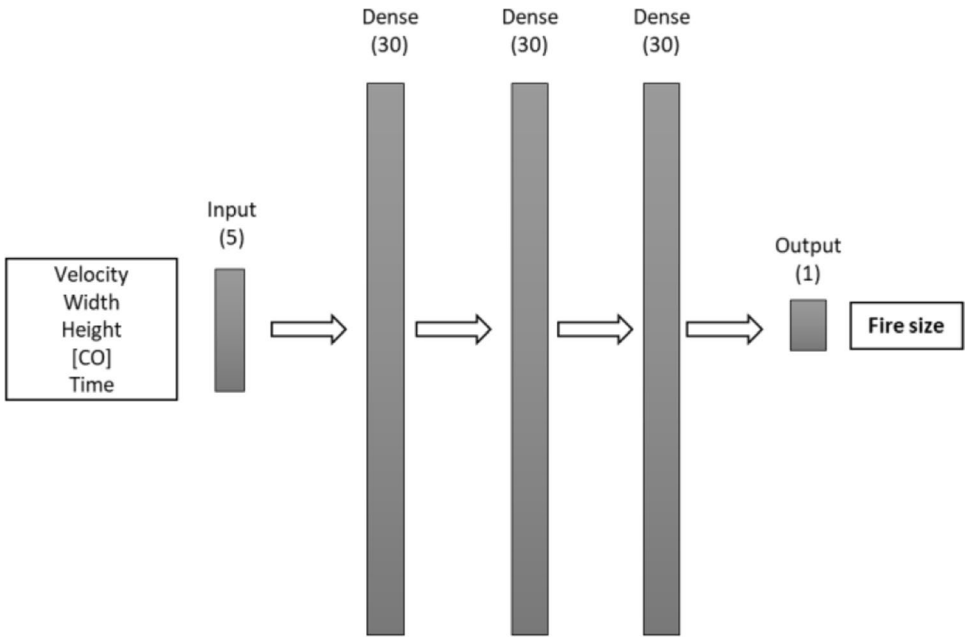

Fig. 2 Architecture of ANN-1

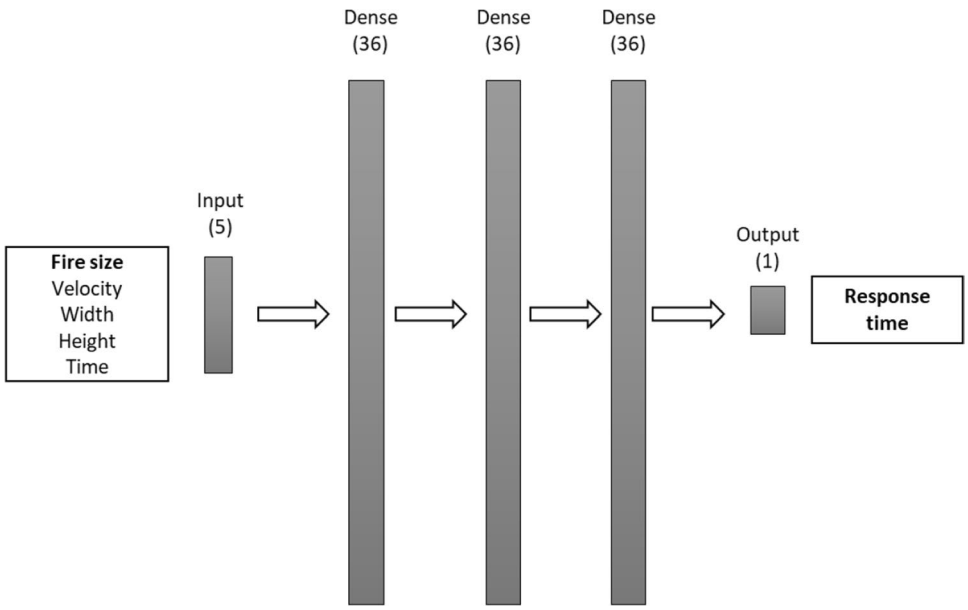

Fig. 3 Architecture of ANN-2

of 5 elements that as mentioned previously corresponds to longitudinal air velocity, tunnel width, tunnel height, CO concentration, and time elapsed after fire detection. The output layer consists of one element that refers to the fire size prediction which is included in the input vector of ANN-2. The architecture of ANN-2 also consists of three hidden layers of 36 neurons for a total of 5 fully connected layers as shown in Fig. 6. The input vector of ANN-2 consists of 5 elements that corresponds to fire size, velocity, tunnel width, tunnel height, and time elapsed after fire detection. In both ANNs, the rectified linear unit activation function (ReLu) was used for the hidden layers. The Adam gradient descent optimization algorithm with the mean squared error as loss function was used. Ten thousand epochs with a batch size of 100 samples and a learning rate fixed at 10^{-2} were used for training both ANNs. All weights and biases were initialized from a normal distribution with zero mean and 10^{-2} standard deviation. The network architecture was created using Keras, a high-level neural network library built-in Python that runs on top of TensorFlow, an open-sourced end-to-end platform [19, 20].

2.2 Tenability Analysis

The tenability analysis allows for the determination of the parameters and limits that should be considered to evaluate the tenability of the conditions in the fire proximity. US mining regulation requires that each operator of an underground coal mine drafts an emergency and firefighting program that guides all miners in the procedure that they must follow if a fire occurs [18]. The regulation stipulates that during a mine fire some miners are designated to respond to the mine fire emergency while other miners are required to evacuate the mine. Mining regulation specifies that at least two miners in each working section and one miner for every four miners on a maintenance shift must be proficient in the use of fire suppression equipment available in the mine and know its location [18]. The underground miners assigned to address the fire are called the first responder group (FRG) since they are the first group to deal with the fire. The FRG is commonly composed of barefaced personnel [2].

In addition to the FRG, there is a second group composed of specially trained fire brigade and mine rescue team called the second responder group (SRG). Although a fire brigade is more focused on firefighting, the mine rescue team may also conduct firefighting activities during rescue procedures. Mining regulation requires every operator of an underground mine shall establish at least two mine rescue teams which are available when miners are underground [18]. The SRG has more specialized personal protective equipment (PPE) such as turnout gear and self-contained breathing apparatus (SCBA). Moreover, this group normally carries firefighting equipment that includes efficient water hose nozzles with pistol grips allowing the members of this group to attack fires with more control of water patterns and flows [2].

The tenability analysis carried out in this study is based on previous tenability analysis performed in road tunnels [21–23] and in a simulated methane fire event at the working face in a coal mine [24]. Following these analyses, four main parameters should be considered during tenability analysis. The parameters are toxicity, temperature, visibility, and radiation. In this study, the data-driven approach was only developed to determine response time for the SRG; thus, temperature, radiation, and visibility were only considered. It is noteworthy that for the SRG the toxicity is not accounted since this group normally carries SCBA designated to provide oxygen for at least 4 h and is suitable for firefighting. In some tenability analyses previously performed, some limits are determined for certain time of exposure such short-term exposure limits (STEL). However, in this study limits were established as ceiling or critical limit as also recommended by Gehandler et al. [22]. In real mine fires and numerical simulations have been observed that when parameters reach numbers close to the exposure limits, it is almost a certainty that they will keep increasing if the fire is not attacked. In addition, visibility is generally the first tenability parameter limit exceeded (well before limits for toxicity, temperature, and radiation) and its limit is always considered a critical limit due to the difficulty that firefighters have performing essential activities such as fire approaching, firefighting, and evacuation. Considering the accessibility of underground coal mines and the remote location of fires, this assumption assures a conservative approach.

The temperature and radiant heat limits for the SRG are determined by Haghighat and Luxbacher [24], and NFPA [21], respectively. Haghighat's work proposed a temperature of 100 °C for SRG wearing turnout gear. NFPA says that for SRG a radiation level under roughly 5 kW/m^2 can be withstood for around 7 min. However, in this study this value was considered the ceiling limit. Regarding visibility, its tenability limit is commonly established based on its impact on firefighters walking speed. Studies have been performed to determine the walking speed in function of the visibility and the extinction coefficient [25]. For purposes of this work, the tenable visibility limit was set to 5 m based on Gehandler et al. [22]. They mentioned that this visibility limit can be set as long as firefighters know the environment where the fire occurs. It is noteworthy that a maximum visibility of 30 m was set in FDS. An optical coefficient equal to 3 [26] was used assuming light reflecting signs hanging on walls that indicate evacuation route as it is common in underground coal mines. Explosibility was not considered in this study; however, if fire firefighters observe or suspect an explosive atmosphere during an ongoing fire (e.g., methane concentration between 5 and 15% with an oxygen concentration between 15 and 20%), the response time must be zero and

Table 1 SRG tenable limits

Parameter	Ceiling limit
Heat flux (kW/m^2)	< 5.0
Temperature (°C)	< 100
Visibility (m)	> 5

the scenario must be considered as not tenable immediately. The tenability limits used in this study are summarized in Table 1.

2.3 Data Generation

As stated previously, the data used to train and test the data-driven approach was generated from numerical simulations. Three hundred fire scenarios in a flat and straight mine entry were simulated in FDS and FSSIM. FDS simulations provided spatial–temporal results to determine the conditions in the fire proximity. FSSIM simulation results were used to determine CO concentration at sensor stations within 300 m downwind from the fire. It is noteworthy that in all scenarios simulated at least one tenability limit was exceeded to determine the response time. Figure 4 shows the locations in which CFD and FSSIM simulations were performed with reference to the fire position.

2.3.1 CFD Data Generation

CFD simulations were carried out to determine the conditions at the attack position using FDS. FDS is a large-eddy simulation model that solves the equations of mass, momentum, energy, and species conservation to determine the conditions due to the evolution of fire, transport of gasses, and smoke in an enclosed space [27]. These equations are solved using the method of finite differences on a collection of uniformly spaced-three-dimensional grids [28] allowing for the predictions of parameters such as combustion gas concentrations, visibility, heat flux, and soot fraction in each grid of the domain.

The geometry used in FDS simulations is shown in Fig. 5. It was assumed that the fire location in these scenarios was located at a belt entry between two crosscuts as shown in Fig. 4. The simulation input parameters varied in this study are shown in Table 2 and highlighted in Fig. 5. These parameters were selected since they have direct influence on the

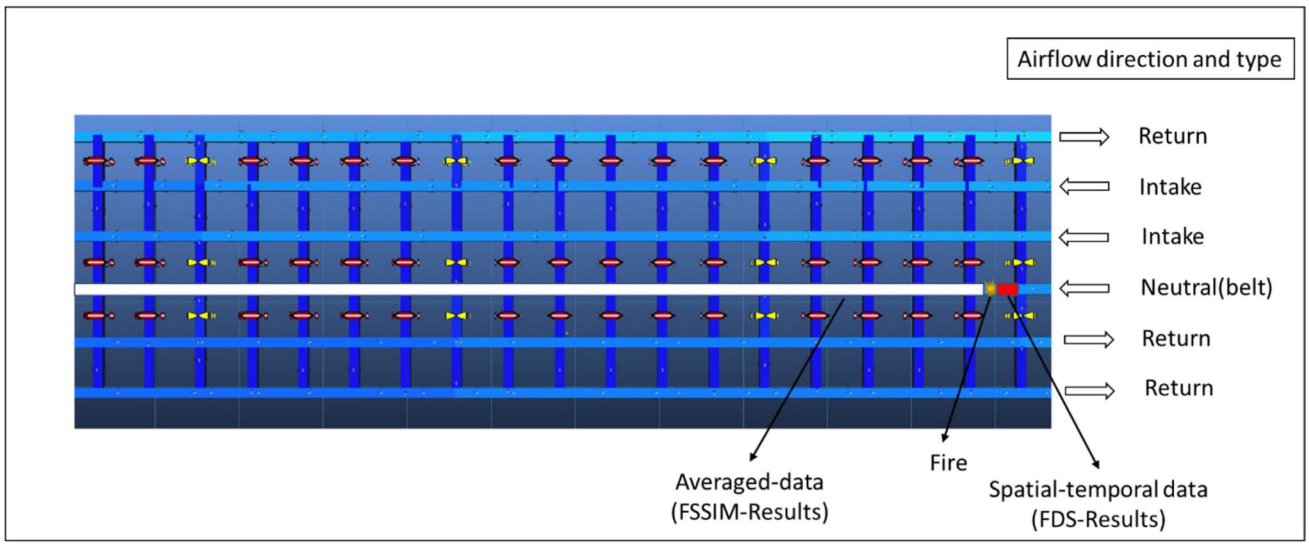

Fig. 4 Locations of FDS and FSSIM results (plan view of mine ventilation schematic)

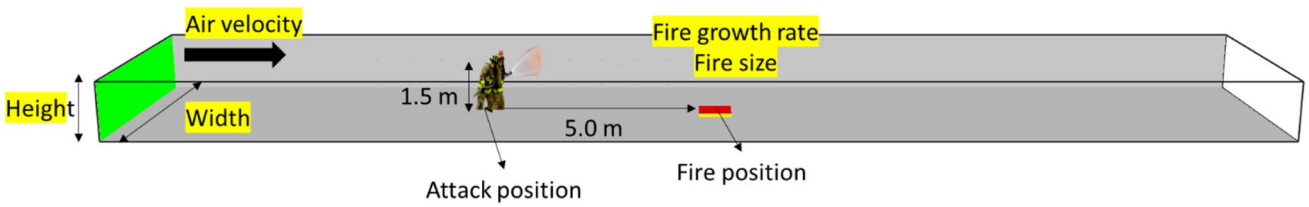

Fig. 5 FDS geometry. Parameters varied in simulations are highlighted

Table 2 Range of each parameter in study

Parameter	Range
Air velocity (m/s)	0.5–2.0
Fire size (kW)	750–7000
Fire growth rate (s^{-1})	0.01172–0.1876
Height	1.8–2.8 m
Width	5.0–7.0 m

presence and amount of backlayering [29–35]. Backlayering is defined as the reversal flow of smoke and combustion gasses within a tunnel (towards the forced ventilation) affects the visibility and toxicity at the attack position leading to untenable conditions. During direct attack, firefighters approach the fire and position themselves approximately 5 m upwind of the fire. At this attack position, they proceed to try and suppress the fire using water or firefighting foam. For this reason, FDS simulations were used to determine the conditions at the attack position assumed to be 5 m away upwind of the fire and at a height of 1.5 m. A height of 1.5 was selected since firefighters would try to crouch when they attack the fire with the objective to stay below the smoke layer as was also assumed by Haghighat and Luxbacher [24].

The values of parameters shown in Table 2 for each scenario were obtained using simple random sampling from uniform distribution in which each value has the same probability of being drawn during the sampling process. However, it was assured that conditions grow untenable for firefighters in all scenarios to determine the response time. The simulation time of the 300 FDS scenarios varied depending on the fire size and growth rate. Each scenario was determined to last until the time the maximum fire size (t_{max}) is reached. The fire size at time (t) was determined using the T-squared approach shown in Eq. 1 for all scenarios.

$$HRR(t) = \alpha t^2 \tag{1}$$

In the above equation, HRR is the fire size at a time (t) and α is the fire growth rate that it is defined as shown in Eq. 1. Note that the lower and upper limits of the fire growth rate range refer to the standard medium and ultrafast growth rates, respectively.

$$\alpha = \frac{HRR_{max}}{{t_{max}}^2} \tag{2}$$

where HRR_{max} is the maximum fire size reached at t_{max}.

The grid size (dx) was 0.1 m along each axis of the domain for all simulations to reduce calculation time and computational cost as well as have consistent results. McGrattan et al. [36] recommend a grid size value less than or equal to $0.1D^*$ to completely resolved the source fire. D^* refers to the characteristic length scale that corresponds to the total HRR of a fire plume defined in Eq. 3. Although the grid size used in this study does not fully resolve the source fire for sizes lower than 1,000 kW, the predictions were adequate for exploratory analysis to test the ability of ANNs to make predictions than comparing to experimental results. The range of D^*/dx is between 21 and 9 for fire sizes of 7000 kW and 500 kW, respectively.

Table 3 Heat of combustion, CO, soot, and CO_2 yields of the material involved in the fire

Material	Heat of combustion (kJ/kg)	Y_{CO} (kg/kg)	Y_{SOOT} (kg/kg)	Y_{CO_2} (kg/kg)
Polyurethane	25,300	0.02775	0.1875	1.5325

$$D^* = \left(\frac{Q}{\rho C_P T_0 \sqrt{g}}\right)^{2/5} \tag{3}$$

where Q is the heat release rate of fire, ρ is the air density, C_P is the air specific heat, T_0 is the ambient temperature, and g is the gravity acceleration.

The parameters shown in Table 1 were determined during the simulations since they allow for the evaluation of conditions for firefighters as detailed in "Sect. 2.2." The value of each parameter was calculated at intervals of 1 s at the attack position. Flexible polyurethane foam was used as the material to simulate the fire in each scenario. Characteristics of flexible polyurethane foam are shown in Table 3.

2.4 Zone Fire Model Data Generation

To determine the CO concentration downwind of the fire, FSSIM was used. In FSSIM, each control volume or compartment is represented as single node. Junctions that represent flow paths are defined between nodes. The approach of just having one node per control volume minimizes the computational cost and time allowing for predictions of smoke spread in larger domains such as large areas in underground coal mines. FSSIM solves the 1-D conservation equations for mass, momentum, and energy [37]. In zone fire models also referred to as a 1D or network fire model, it is assumed that properties such as temperature, density, and chemical species take constant values through each zone.

A previous study carried out by Haghighat et al. [38] shows that 1D fire model results normally have an error of less than 5% when compared with CFD model results for zones of the domain located 12 times the hydraulic diameter (Dh) farther away downstream from the fire. Farther this distance known as the downstream interface boundary, the fluid field behaves as a quasi-1D fluid dominated by the longitudinal velocity. This finding allows for using 1D models

such as FSSIM in parametric studies as the presented in this work to predict fire conditions at a low computational cost and time in large tunnel domains. While the calculation time for a 1D fire simulation in a 400 m long tunnel can take around 30 min using a single NVIDIA Quadro K620 graphics, the calculation for a CFD fire model can be in the order of 2 weeks.

The 300 scenarios simulated in FDS were also simulated in FSSIM using the same input parameters and fuel characteristics shown in Table 2 and Table 3, respectively. FSSIM simulations were used to determine the CO concentrations within 300 m downwind from the fire in each scenario. The downwind CO concentration was determined at intervals of 1 s at 4 different sensor stations with a spacing of 75 m as shown in Fig. 6. The geometry used in FSSIM consisted of a flat and straight mine entry 400 m long and split into 80 compartments. Thus, the length of the compartments was 5 m. The tunnel height and width depended on the mine entry dimensions of each scenario. The fire was located 17.5 m away from the inlet. The maximum CO concentration detected at the sensor stations at each time step was used as input parameter in the data-driven approach. Two air leakages along the tunnel were considered based on the location of crosscuts downwind from the fire as shown in Fig. 6. The airflow quantities at leakage points were calculated based on mine survey results from a partner mine.

2.5 Data Preparation

During the data preparation, simulation input parameters and numerical results of FDS and FSSIM were processed with the objective of being used for training and testing the ANNs and the entire model (interconnected ANNs). The first step consisted of linking input parameters with FDS and FSSIM results. This can be done because same scenarios were simulated in both models. With the objective to be more illustrative with the linking process, the linking of three samples of scenario A shown in Table 4 is detailed in what follows. Based on time elapsed and fire size, it was possible to link tenability parameter results at the attack position predicted by FDS with the CO concentration downwind from the fire predicted by FSSIM. This is possible since time elapsed and fire size are equally predicted at any time in both fire models as shown under FDS/FSSIM column in Table 4.

Once input parameters and results of both models were linked, the maximum response time for each scenario was calculated. This time was determined by looking for the time in which at least one of tenability limit was exceeded in each scenario. For instance, in scenario A the maximum response time was determined at 466 s when the tenability limit of visibility was exceeded. It is called maximum response time because it is referenced from the fire detection time ($t = 0$ s). Then, in order to determine the response time for each time step associated with the CO concentration and the other input parameters (tunnel dimensions, air velocity, and time elapsed), the value of maximum response time was subtracted by the value of each time step. After calculation of response time for each time step, the inputs and outputs of the models were assigned. Tables 5, 6, and 7 show the values of the input and output parameters for the first and second ANNs, and the entire model (interconnected ANNs) based on results of scenario A shown in Table 4, respectively.

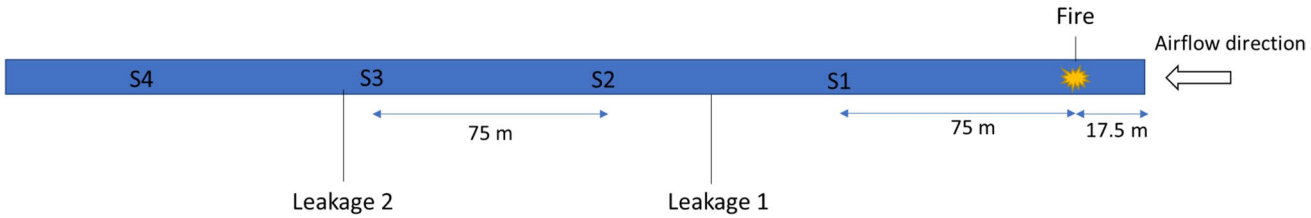

Fig. 6 Geometry used in FSSIM, location of sensor stations, fire, and leakages

Table 4 Input parameters and results of both fire models linked for three different time steps of Scenario A

Scenario	Simulation input parameters				FDS/FSSIM		FDS		FSSIM
	Vel (m/s)	Max fire size (kW)	Growth rate (s^{-1})	Dim (H×W) (m×m)	Current fire size (kW)	Time (s)	**Temp (°C)**	Visibility (m)	[CO] (ppm)
A	1.4	5182	0.012	2.8×6.2	450	194	20	30	5
A					747	250	21	30	10
A					2594	465	43	6	42

Table 5 Values of input and output parameters of the ANN-1 for three samples of scenario A

Scenario	Inputs					Output
	Time (s)	[CO] (ppm)	Vel (m/s)	Height (m)	Width (m)	Fire size (kW)
A	194	5	1.4	2.8	6.2	450
A	250	10	1.4	2.8	6.2	747
A	465	42	1.4	2.8	6.2	2594

Table 6 Values of input and output parameters of the ANN-2 for the three samples of scenario A

Scenario	Inputs					Output
	Time (s)	Fire size (kW)	**Vel (m/s)**	**Height (m)**	**Width (m)**	**Response time (s)**
A	194	450	1.4	2.8	6.2	272
A	250	747	1.4	2.8	6.2	216
A	465	2594	1.4	2.8	6.2	1

Table 7 Values of input and output parameters of the entire model (two interconnected ANNs) for three samples of scenario A

Scenario	Inputs					Output
	Time (s)	[CO] (ppm)	Vel (m/s)	Height (m)	Width (m)	Response time (s)
A	194	5	1.4	2.8	6.2	272
A	250	10	1.4	2.8	6.2	216
A	465	42	1.4	2.8	6.2	1

3 Results and Discussion

After processing 300 simulation results from FDS and FSSIM, 24,694 samples were collected for training and testing ANNs and testing the entire model. The entire dataset was randomly split into two, with 80% for training and 20% for testing. The ANNs were trained independently using the training data. The performance of ANN-1, ANN-2, and the entire model on each dataset was determined. ANN-1 was tested based on fire size predictions. ANN-2 and the entire model were tested based on response time predictions. During the performance evaluation of the entire model, inputs of ANN-1 were feed to the entire model and error for response time predictions was determined.

In order to determine the performance of ANN-1, the error for fire size predictions was calculated as follows:

$$E_{FS,ANN1} = FS_T - FS_{ANN-1} \tag{4}$$

where $E_{FS,ANN1}$ is the error for fire size, FS_T is the true fire size, and FS_{ANN-1} is the fire size predicted by ANN-1.

In the same way, for the determination of the performance of ANN-2 and the entire model, the error for response time was calculated as follows:

$$E_{RT,ANN2} = RT_T - RT_{ANN-2} \tag{5}$$

$$E_{RT,MODEL} = RT_T - RT_{MODEL} \tag{6}$$

where $E_{RT,ANN2}$ is the error for response time when ANN-2 is evaluated, RT_T is the true response time, RT_{ANN-2} is the response time predicted by ANN-2, $E_{RT,MODEL}$ is the error for response time when the entire model is evaluated, and RT_{MODEL} is the response time predicted by the entire model.

Due to the fluctuations inherent to the turbulent flow in FDS simulation, FDS results were processed applying an average filter with a window of 15 s in order to reduce the noise of the data. Figure 7 shows the evolution of visibility over time for scenario A before and after applying the average filter.

The discrete probability density function of fire size error (ANN-1) and response time error (ANN-2) for all training and test data when ANNs were evaluated independently are shown in Figs. 8 and 9, respectively. Figure 10 shows the discrete probability function of response time error when the entire model was used for all training and test data. The mean and standard deviation of error predictions of ANN-1, ANN-2, and the entire model are summarized in Table 8. An error of zero indicates perfect agreement between the ANN predictions and true values obtained from fire models.

Table 8 shows that the mean fire size error of ANN-1 is − 1.61 kW with a standard deviation of 12.97 kW for training set and a mean fire size error of − 1.69 kW with a standard deviation of 14.36 kW for the test set. Based on this result, it can be stated that 95% of ANN-1 predictions should be within ± 29 kW which highlight the capability of ANN-1 to predict the current fire size only using available information during ongoing mine fires. However, much of the fire size error in ANN-1 predictions was identified to come from two sources. The first source was related with the

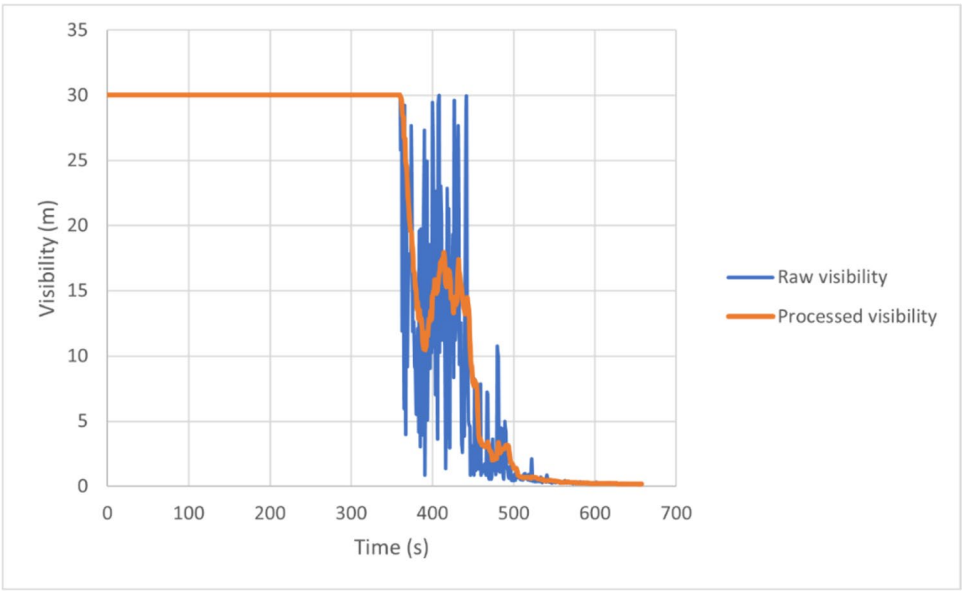

Fig. 7 Raw and visibility over time for scenario A

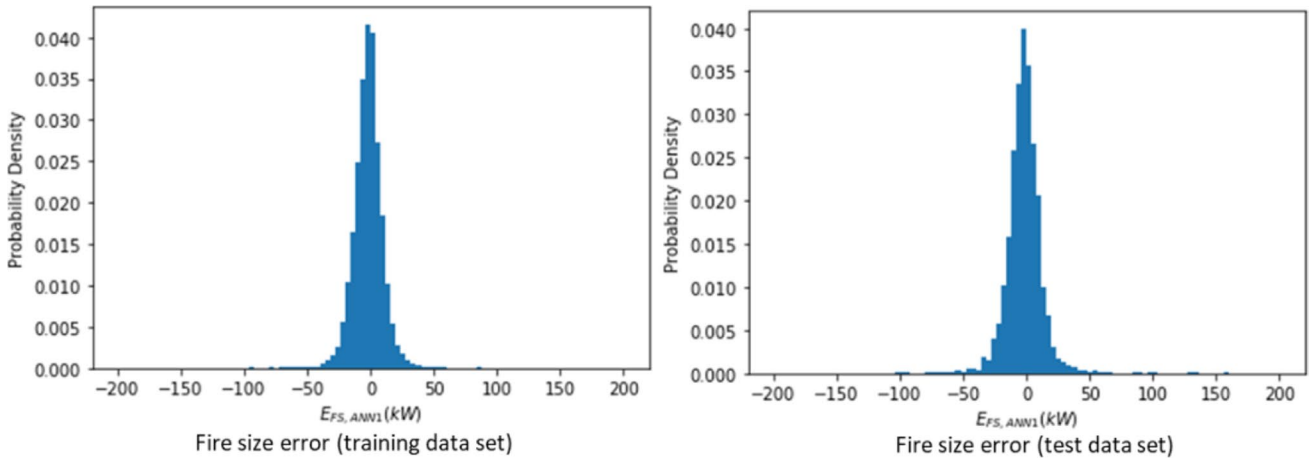

Fig. 8 Discrete probability density functions of ANN-1 error from training and testing dataset

evolution of the fire size is not immediately reflected in the variation of the CO concentration measured by the sensors downwind from the fire. The longitudinal air velocity of each scenario has a significant influence on the CO concentration travel time from the source to the sensor locations. There is a velocity range in which ANN-1 performs well: however, for lower or higher velocities in this range, ANN-1 becomes less accurate. In addition to air velocity, different flowrates produce more diluted or higher CO concentration downwind from the fire. These two parameters cause a wide variability in the data that cannot be completely captured by ANN-1 with the input parameters used. In order to determine the relationship between ANN-1 performance and air velocity, the mean fire size error and standard deviation for scenarios with different air velocities were determined as shown in Table 9. Table 9 shows that the best performance of ANN-1 is when fire size is predicted for samples of scenarios with velocity between 1.0 and 1.5 m/s. The lowest mean fire size error and standard deviation were evidenced in this range. On the other hand, greater mean fire size errors and standard deviations were seen for scenarios with air velocity in the range of 0.5–1.0 m/s and 1.5–2.0 m/s.

The second error source is related to the number of samples in each velocity range. Table 9 shows that higher errors were obtained for velocity ranges with lower number of samples. The low number of samples in the velocity range of 0.5 and 1.0 m/s is explained due to the short time in which the conditions are tenable at the attack position. The response time for scenarios with lower air velocities generally is short; thus, the number of samples generated in those scenarios

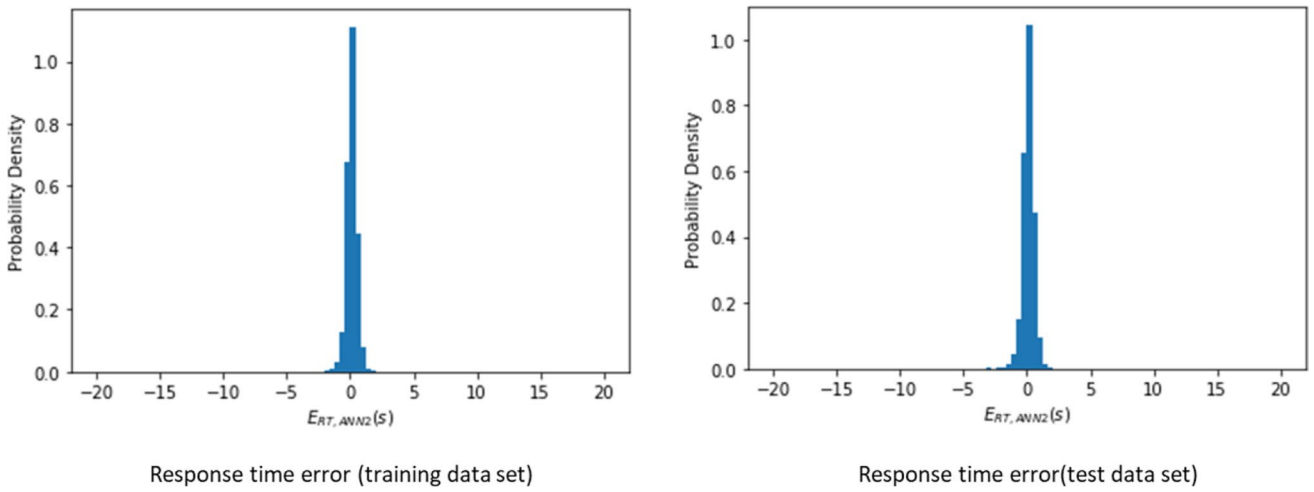

Fig. 9 Discrete probability density functions of ANN-2 error from training and testing dataset

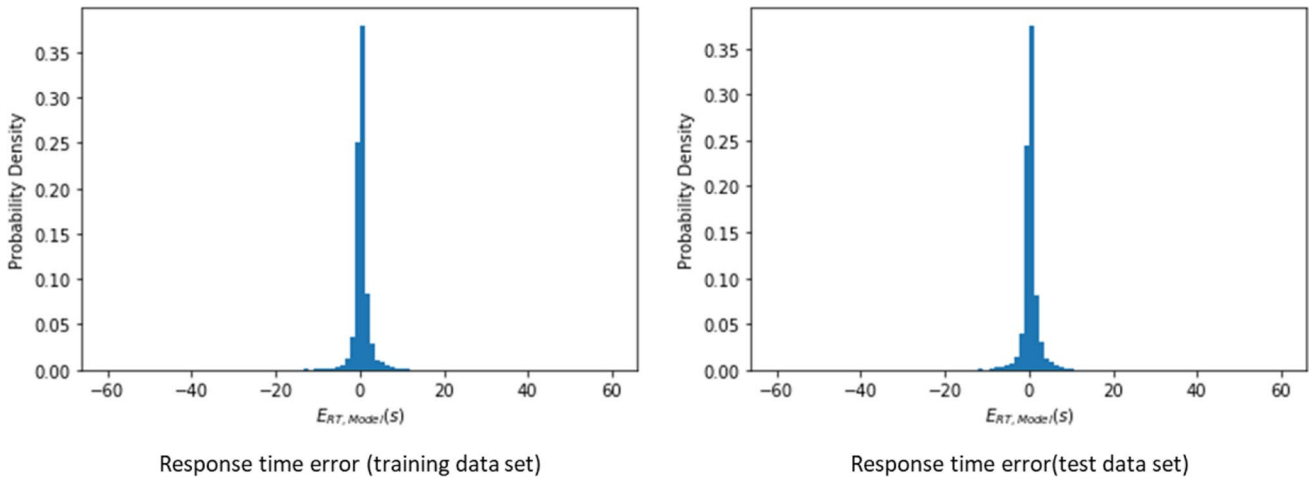

Fig. 10 Discrete probability density functions of the entire model error from training and testing dataset

Table 8 Summary of performance of ANN-1, ANN-2, and entire model on training and test data (values refers to $\mu \pm 2\sigma$)

Model	Prediction	Training set error	Test set error	Unit
ANN-1	Fire size	-1.61 ± 12.97	-1.69 ± 14.36	kW
ANN-2	Response time	0.13 ± 0.40	0.13 ± 0.43	s
Entire model	Response time	-0.36 ± 1.80	-0.33 ± 1.84	s

Table 9 Summary of performance of ANN-1 and number of samples for different velocity ranges

Velocity range (m/s)	Error ($\mu \pm 2\sigma$)	Number of samples
0.5–1.0	-2.18 ± 19.75	4818
1.0–1.5	-0.63 ± 10.43	14,043
1.5–2.0	-3.6 ± 12.38	5833

is smaller. Regarding the number of samples generated in scenarios in the velocity range of 1.5 and 2.0 m/s can be stated that the small number of samples is explained due to the lower number of scenarios with these velocities in which the tenability limits are exceeded. Scenarios with greater air velocities require larger fire sizes to grow untenable conditions for firefighters.

Two approaches may be considered to reduce ANN-1 error. The first approach is including more training data that increases the number of samples for the previously mentioned velocity ranges. The second approach is adding other input parameters that provide more information related to the fire evolution such as the maximum fire size or fire growth rate, but these parameters are not available

or measurable during mine fires. Based on results shown in Table 8, the desired performance of ANN-1 is met considering the limitations in the availability of parameters during the mine fire emergency.

Regarding ANN-2, Table 8 shows that the mean response time error of ANN-2 is − 0.13 s with a standard deviation of 0.40 s for the training set and a mean response time error of 0.13 s and standard deviation of 0.43 s for testing set. Based on these values, it can be stated that the 95% of ANN-2 predictions should be within ± 1.0 s when the true fire size is used as input parameter. These results highlight the capability of ANN-2 to predict response times with high degree of accuracy when the true or actual fire size is used. The use of the actual fire size along with the other input parameters provide enough information to ANN-2 to capture data variability for having response time predictions with low error values.

The mean response time error of the entire model is − 0.36 s with a standard deviation of 1.80 s for the training set. The mean response time error of the entire model is − 0.33 s with a standard deviation of 1.84 s for the testing set. As mentioned previously, the input parameters from datasets were feed to ANN-1 and error was determined from response time predictions by ANN-2. This indicates that the fire size error of ANN-1 propagates to ANN-2 and explains why the entire model error is greater than ANN-2 error for response time predictions. Even though errors of fire size predictions by ANN-1 affect the performance of the entire model, 95% of the entire model predictions of response time should be within ± 4.0 s when available input parameters during underground coal mine fires are used.

4 Conclusion

A data-driven approach was presented to predict fire size and response time in real time for firefighters based on available and measurable input parameters during ongoing mine fires using two interconnected feedforward ANNs. The data for training and testing the ANNs were generated from 300 scenarios with different longitudinal air velocities, mine entry dimensions, and fire characteristic simulated in FDS and FSSIM. Simulations in the FDS model allowed for the determination of the conditions at the attack position assigned to be 5.0 m upwind from the fire. Simulations in FSSIM allowed for establishing the CO concentration evolution within 300 m downwind from the fire. After linking input parameters and simulation results from both models, 24,694 samples were collected of which 80% was used for training and 20% was used for testing the robustness of the approach.

Results showed that 95% of fire size predictions were within ± 29 kW of the true fire size, and 95% of response time predictions were within ± 4.0 s of the true response time when testing data was used. The major fire size error was identified to come from predictions for samples with air velocities within 0.5–1.0 m/s and 1.5–2.0 m/s ranges. The variability in data caused by different air velocities and flowrates it is not entirely provided by input parameters of ANN-1. In addition, the small number of samples for these velocity ranges could be another cause of the fire size error. The largest response time error can be attributed to inaccuracies in the fire size predictions since when ANN-2 was tested using true fire sizes, the response time error was much lower. Thus, it can be stated that the fire size error of ANN-1 propagates to ANN-2 as fire size predicted by ANN-1 is used as input in ANN-2.

This work demonstrates that using available and measurable input parameters during ongoing mine fires in the data-driven approach is possible to determine the fire size and response time in real time. While the model presented in this work was designed for a belt entry, the same methodology could be implemented in other mine locations. Additionally, this approach could be applied in different enclosed locations such as underground storage facilities and road tunnels where parameters collection can be performed from high-tech electrical devices such as heat-cameras not allowed in underground coal mines. Thus, more complex data-driven approaches that use image processing techniques could be developed. Finally, future work is needed to incorporate additional physics components such as different fuels and reaction parameters that have direct influence on the conditions during mine fires to provide broader and more realistic input to emergency situations.

Acknowledgements The findings and conclusions in this report are those of the authors and do not reflect the official policies of the Department of Health and Human Services; nor does mention of trade names, commercial practices, or organizations imply endorsement by the US Government.

Funding This research was funded by the National Institute Safety and Health (NIOSH) under Contract No. 200–2014-59669.

Data Availability All datasets and codes used for supporting the conclusions of this article are available upon request at the following website: https://drive.google.com/drive/folders/1KEGBPD46T2B8PGabhVTkqL9CrAxHw1nR?usp=sharing

Declarations

Conflict of Interest The authors declare no competing interests.

References

1. Conti RS, Chasko LL, Wiehagen WJ, and Lazzara CP (2000) "An underground coal mine fire preparedness and response checklist: the instrument," Pittsburgh, PA

2. Conti RS, Chasko LL, Wiehagen WJ, and Lazzara CP (2005) "Fire response preparedness for underground mines," Pittsburgh, PA
3. Trevits MA, Yuan L, Teacoach K, Valoski MP, Urosek JE (2009) "Understanding mine fires by determining the characteristics of deep-seated fires," in SME Annual Conference
4. Brake DJ (2013) "Fire modelling in underground mines using Ventsim visual VentFIRE software,". The Australian mine ventilation conference
5. Yu LX, Beji T, Maragkos G, Liu F, Weng MC, Merci B (2018) Assessment of numerical simulation capabilities of the fire dynamics simulator (FDS 6) for planar air curtain flows. Fire Technol 54(3):583–612. https://doi.org/10.1007/s10694-018-0701-7
6. Kerber S, Milke JA (2007) Using FDS to simulate smoke layer interface height in a simple atrium. Fire Technol 43(1):45–75. https://doi.org/10.1007/s10694-007-0007-7
7. Hadjisophocleous G, Jia Q (2009) Comparison of FDS prediction of smoke movement in a 10-storey building with experimental data. Fire Technol 45(2):163–177. https://doi.org/10.1007/s10694-008-0075-3
8. Shen TS, Huang YH, Chien SW (2008) Using fire dynamic simulation (FDS) to reconstruct an arson fire scene. Build Environ 43(6):1036–1045. https://doi.org/10.1016/j.buildenv.2006.11.001
9. Salem AM (2013) Parametric analysis of a cabin fire using a zone fire model. Alexandria Eng J 52(4):627–636. https://doi.org/10.1016/j.aej.2013.10.001
10. Peacock RD, Forney GP, and Reneke PA (2015) "NIST technical note 1889v3 CFAST – consolidated fire and smoke transport (version 7) volume 3 : verification and validation guide," 3 7 https://doi.org/10.6028/NIST.TN.1889v2
11. Buffington T, Cabrera JM, Kurzawski A, Ezekoye OA (2020) Deep-learning emulators of transient compartment fire simulations for inverse problems and room-scale calorimetry. Fire Technol. https://doi.org/10.1007/s10694-020-01037-2
12. Lee J, Lee S, and You D (2018) "Deep learning approach in multi-scale prediction of turbulent mixing-layer," 1–21.https://doi.org/10.48550/arXiv.1809.07021
13. Lee S, and You D (2017) "Prediction of laminar vortex shedding over a cylinder using deep learning," no. Wu 2011.https://doi.org/10.48550/arXiv.1712.07854
14. Miyanawala TP, and Jaiman RK (2017) "An efficient deep learning technique for the Navier-Stokes equations: application to unsteady wake flow dynamics,".https://doi.org/10.48550/arXiv.1710.09099
15. Raissi M, Yazdani A, and Karniadakis GE (2018) "Hidden fluid mechanics: a Navier-Stokes informed deep learning framework for assimilating flow visualization data,".https://doi.org/10.48550/arXiv.1808.04327
16. Maulik R, San O (2017) A neural network approach for the blind deconvolution of turbulent flows. J Fluid Mech 831:151–181. https://doi.org/10.1017/jfm.2017.637
17. Hodges JL, Lattimer BY, Luxbacher KD (2019) Compartment fire predictions using transpose convolutional neural networks. Fire Saf J 108(November 2018):102854 2019. https://doi.org/10.1016/j.firesaf.2019.102854
18. US Code of Federal Regulations (2016) CFR, title 30 (mineral resources) part 75. Mandatory safety standards—*underground coal mines*. United States. https://www.ecfr.gov/current/title-30/chapter-I/subchapter-O/part-75?toc=1
19. M. Abadi et al. (2016) "TensorFlow: large-scale machine learning on heterogeneous distributed systems,"
20. F. Chollet, "Keras," GitHub repository, 2015. [Online]. Available: https://www.github.com/fchollet/keras
21. NFPA (2020) NFPA 502:standard for road tunnels, bridges, and other limited access highways
22. Gehandler J, Ingason H, Lönnermark A, Frantzich H, and Strömgren M (2013) Performance-based requirements and recommendations for fire safety in road tunnels (FKR-BV12)
23. Ingason H, Li YZ, and Lönnermark A (2015) "Tunnel fire ventilation," in Tunnel fire dynamics, 53, 9, New York, NY: Springer New York, 333–360.
24. Haghighat A, Luxbacher K (2018) Tenability analysis for improvement of firefighters' performance in a methane fire event at a coal mine working face. J Fire Sci 36(3):256–274. https://doi.org/10.1177/0734904118767066
25. Fridolf K, Andrée K, Nilsson D, Frantzich H (2014) The impact of smoke on walking speed. Fire Mater 38(7):744–759. https://doi.org/10.1002/fam.2217
26. McGrattan K, Hostikka S, Floyd J, Mcdermott R, Weinschenk C, and Overholt K (2016) Sixth edition fire dynamics simulator user's guide, 1019
27. McGrattan KB, Mcdermott R, Hostikka S, Floyd J, Weinschenk C, Overholt K (2016) Fire dynamics simulator user's guide. Gaithersburg, MD
28. McGrattan K, Hostikka S, McDermott R, Floyd J, Weinschenk C, and Overholt K (2015) "Fire dynamics simulator technical reference guide volume 1: mathematical model (sixth edition). NIST Spec Publ 1018 1
29. Li YZ, Ingason H (2017) Effect of cross section on critical velocity in longitudinally ventilated tunnel fires. Fire Saf J 91(May):303–311. https://doi.org/10.1016/j.firesaf.2017.03.069
30. Li YZ, Lei B, Ingason H (2010) Study of critical velocity and backlayering length in longitudinally ventilated tunnel fires. Fire Saf J 45(6–8):361–370. https://doi.org/10.1016/j.firesaf.2010.07.003
31. Oka Y, Atkinson GT (1995) Control of smoke flow in tunnel fires. Fire Saf J 25(4):305–322. https://doi.org/10.1016/0379-7112(96)00007-0
32. Thomas PH (1958) "The movement of buoyant fluid against a stream and the venting of underground fires" Fire Res Stn351
33. Thomas PH (1968) "The movement of smoke in horizontal passages against an air flow.," Fire Res Stn 723
34. Vauquelin O (2005) Parametrical study of the back flow occurrence in case of a buoyant release into a rectangular channel. Exp Therm Fluid Sci 29(6):725–731. https://doi.org/10.1016/j.expthermflusci.2005.01.002
35. Wu Y, Bakar MZA (2000) Control of smoke flow in tunnel fires using longitudinal ventilation systems - a study of the critical velocity. Fire Saf J 35(4):363–390. https://doi.org/10.1016/S0379-7112(00)00031-X
36. McGrattan K, Baum H, Rehm R (1999) Large eddy simulations of smoke movement. ASHRAE Trans 105:426
37. Floyd JE, Hunt SP, Williams FW, and Tatem PA (2005) A network fire model for the simulation of fire growth and smoke spread in multiple compartments witcomplex ventilation 15. https://doi.org/10.1177/1042391505051358
38. Haghighat A, Luxbacher K, Lattimer BY (2018) Development of a methodology for interface boundary selection in the multi-scale road tunnel fire simulations. Fire Technol 54(4):1029–1066. https://doi.org/10.1007/s10694-018-0724-0